

Green Chemistry

Accepted Manuscript

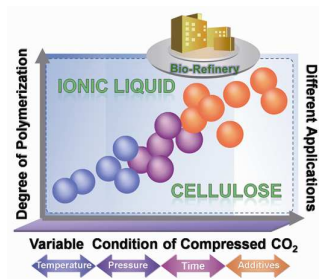


This is an *Accepted Manuscript*, which has been through the Royal Society of Chemistry peer review process and has been accepted for publication.

Accepted Manuscripts are published online shortly after acceptance, before technical editing, formatting and proof reading. Using this free service, authors can make their results available to the community, in citable form, before we publish the edited article. We will replace this *Accepted Manuscript* with the edited and formatted *Advance Article* as soon as it is available.

You can find more information about *Accepted Manuscripts* in the [Information for Authors](#).

Please note that technical editing may introduce minor changes to the text and/or graphics, which may alter content. The journal's standard [Terms & Conditions](#) and the [Ethical guidelines](#) still apply. In no event shall the Royal Society of Chemistry be held responsible for any errors or omissions in this *Accepted Manuscript* or any consequences arising from the use of any information it contains.



Using compressed CO₂ can provide us an easy and sustainable method for staged regeneration of cellulose from ionic liquid.

Cite this: DOI: 10.1039/c0xx00000x

www.rsc.org/xxxxxx

ARTICLE TYPE

Studies on staged precipitation of cellulose from ionic liquid by compressed carbon dioxide

Xiaofu Sun,^a Yanling Chi^b and Tiancheng Mu^{*a}*Received (in XXX, XXX) Xth XXXXXXXXXX 20XX, Accepted Xth XXXXXXXXXX 20XX*

DOI: 10.1039/b000000x

An efficient method to precipitate and refine cellulose from ionic liquid (IL) using compressed CO₂ as gas anti-solvent was proposed. 1-butyl-3-methylimidazolium acetate ([Bmim]OAc) was used as the solvent of microcrystalline cellulose (MCC). The yield and degree of polymerization (DP) value of the regenerated cellulose can be finely tuned by control of the temperature, pressure, reaction time and addition of aprotic polar solvents. For better understanding the possible cellulose precipitation mechanism, the possible carboxylation reaction, volume expansion and solvatochromic parameters of the solution caused by compressed CO₂ were investigated. The solvent strength of the system can be adjusted by the pressure and temperature of CO₂. The regenerated cellulose samples from [Bmim]OAc by addition of different anti-solvents were characterized by solid-state cross-polarization/magic angle spinning (CP/MAS) ¹³C NMR, X-ray diffraction (XRD) spectra and atomic force microscope (AFM). In addition, the energy consumption analysis during anti-solvent process was discussed. The precipitation and staged bio-refinery cellulose from IL is easy, sustainable and cost-efficient.

Introduction

Biomass, mainly consists of polymers and oligomers, is abundant, biodegradable and biocompatible. With the increasing environmental pollution issues and decreasing fossil fuel resources, producing bio-fuels and chemicals using biomass is one of the inevitable trends of the chemical industry development.¹⁻⁵ A series of chemicals such as fuels, solvents, paints and fibers can be obtained by refining the biomass.⁶⁻¹² The efficient separation of the biomass products with different types is significant in the process of bio-refinery.¹³⁻¹⁵ Especially for the biomacromolecules, the degree of polymerization (DP) is one of the critical factors, which affects the property of polymers. As the most abundant natural polymeric compound, cellulose and its derivatives have been widely applied in making paper, plastic, membranes, medicines, and various fabrics and fibers due to the extensive polydispersity.¹⁶⁻¹⁷

Generally, the dissolution of cellulose by disruption of numerous inter- or intra-molecular hydrogen bonds is a prerequisite when processing it to desired products.¹⁸⁻²⁰ Since the 1970s, only a limited number of solvent systems, including LiCl/*N,N*-dimethylacetamide (DMAc), LiCl/*N*-methyl-2-pyrrolidone (NMP), LiCl/1,3-dimethyl-2-imidazolidinone (DMI), dimethyl sulfoxide (DMSO)/tetrabutyl ammonium fluoride (TBAF), *N*-methylmorpholine-*N*-oxide (NMMO), some molten salt hydrates, such as LiClO₄·3H₂O, LiSCN·2H₂O, and some aqueous solutions of metal complexes have been sought to dissolve cellulose.²¹⁻²⁴ However, these solvent systems could result in solvent recovery difficulty and environmental pollution. Compared with the conventional organic solvents, room-

temperature ionic liquids (ILs), containing only ions and generally having a melting point below 100 °C, have been considered as green solvents mainly due to the negligible vapor pressure, high thermal and chemical stability, and their outstanding solvation potential.²⁵⁻²⁹ More importantly, ILs can be tuned to obtain desired property by different combinations of anion and cation. So ILs have been suggested to replace volatile organic compounds in many fields, including in cellulose dissolution processes.^{19, 30-36}

However, the cellulose dissolution by ILs still has drawbacks such as the difficulty of cellulose separation and purification. For cellulose, both the dissolution and the regeneration from solution systems are important. Up to date, the anti-solvent method using molecular solvent shows great advantage in the separation of cellulose from ILs.^{19, 21, 37-39} Briefly, water and ethanol can be added to a binary solution, and the interactions between solute, solvent and anti-solvent make the solubility of the cellulose reduced. Although the solute can be separate out, the problem of the separation of molecular solvent and IL is still needed to solve. In the meantime, the staged bio-refinery of cellulose cannot come true. Therefore, developing less energy consuming, more environmentally friendly, and highly efficient methods for the regeneration cellulose from IL are necessary.

Compressed CO₂ is cheap, nontoxic, nonflammable, and quite soluble in various organic solvents. Many solutes are soluble in organic solvents but not in CO₂ and it can be easily removed by depressurization.⁴⁰⁻⁴¹ Thus the CO₂ can act as a gas anti-solvent (GAS). Many GAS processes, such as extraction and fractionation, recrystallization of chemicals, and micronization have been explored.⁴²⁻⁴⁶ Very recently, we have explored and

reported the recovery of chitosan from its IL solution by compressed CO₂ and found that chitosan micro-particles could be utilized as a catalyst in the reaction of forming imines more efficiently.⁴⁷ Barber *et al.*⁴⁸ have shown that the reaction of 1-ethyl-3-methylimidazolium acetate ([Emim]OAc) and CO₂ may occur with the formation of the carboxylate zwitterion, leading to coagulate chitin and cellulose from IL. The CO₂ anti-solvent method is environmentally benign, which makes the post-processing easier in comparison with the conventional additives that usually cause new issues in the separation process. In addition, the properties of the liquid solvents or the solute molecules can be tuned *in situ* by controlling the pressure and temperature of CO₂.⁴⁹⁻⁵²

In this study, the precipitation of cellulose from IL using compressed CO₂ as anti-solvent to obtain the products with different DP values was investigated. 1-butyl-3-methylimidazolium acetate ([Bmim]OAc) was used as the solvent of microcrystalline cellulose (MCC) for its excellent ability of dissolving cellulose. By control of the temperature, pressure, reaction time and addition of co-solvent, the yield and DP values of the regenerated cellulose can be tuned finely. The solvation of CO₂ in [Bmim]OAc and the possible carboxylation reaction have been investigated by ¹H, ¹³C and ¹⁵N NMR spectroscopy. The effects of volume expansion and solvatochromic parameters of these systems by compressed CO₂ were also investigated to explore the possible anti-solvent precipitation mechanism. In addition, the regenerated cellulose samples from the IL by different anti-solvents were characterized by solid-state cross-polarization/magic angle spinning (CP/MAS) ¹³C NMR, X-ray diffraction (XRD) spectra and atomic force microscope (AFM). Finally, the analysis of energy consumption during different anti-solvent process was discussed and it shows that using compressed CO₂ is more energy-efficient than using conventional high boiling-point solvents.

Results and discussion

Cellulose precipitation performance using compressed CO₂

As is known in previous reports,⁵³⁻⁵⁴ MCC can be directly dissolved in acetate-based ILs and then ethanol can act as anti-solvent in separating it from IL. Our experimental results showed that the DP values of the native and the regenerated cellulose via ethanol were 282 and 163, respectively. The regenerated cellulose sample exhibits a lower DP value after dissolving at high temperature for a long time, which indicates that hydrogen bonds in the cellulose have been disrupted partially and cellulose degradation has occurred in the dissolution process.^{1, 55} Very recently, Barber *et al.*⁴⁸ explored CO₂ could be used as a coagulation solvent for biopolymer-IL solution. CO₂ is miscible with [Bmim]OAc and immiscible with cellulose, which is suitable as an anti-solvent for separation of cellulose and IL. Fig. S1 indicated that when the MCC/[Bmim]OAc system was exposed to compressed CO₂ for a period of time, the cellulose precipitated as a transparent gel after depressurization and removal of CO₂.

In this part, the performance of the compressed CO₂ on the precipitation of cellulose was discussed in detail. Fig. 1 shows that the regenerated cellulose yield increases at a relatively slower rate and reaches the maximum at a reaction time of about 3 h at

6.60 MPa and 25 °C, and about 60 % of regenerated cellulose can be obtained by using compressed CO₂ under this condition. The DP value of the regenerated cellulose also shows a decrease trend and tends to be stable in 3 h. For example, when the regenerated cellulose samples were obtained from compressed CO₂ for 1 h, 2 h, and 3 h, the DP values are 217, 208, and 202 respectively, which were much lower than the native cellulose (DP=282) and a higher than the regenerated one by ethanol (DP=163). It indicates that compressed CO₂ cannot make cellulose recover completely in a short time. Obviously, the cellulose sample with a long chain could be easily influenced by the anti-solvent interaction of compressed CO₂. However, by control of the reaction time of compressed CO₂, as well as the pressure and temperature, we can precipitate cellulose with a specific DP value and narrow molecular weight distribution from [Bmim]OAc.

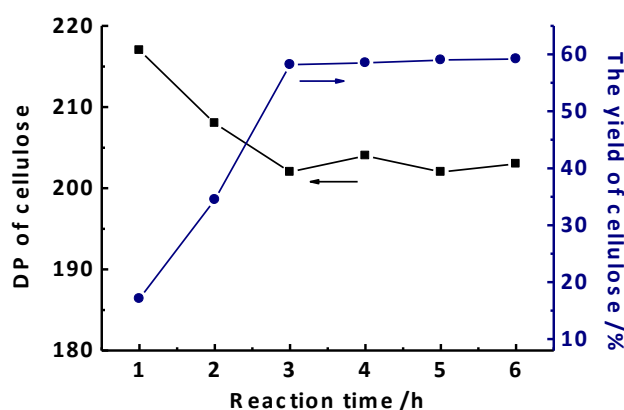


Fig. 1 The DP value and yield of the regenerated cellulose obtained by using compressed CO₂ (25°C, 6.60 MPa) as anti-solvent in different reaction time.

It is worth to consider that if we adjust the pressure of CO₂, the yield of the regenerated cellulose might be changed and the cellulose with different DP values should be staged finely. To affirm this opinion, compressed CO₂ with different pressure were added to the cellulose/[Bmim]OAc systems for 3 h at 25 °C. Fig. 2 shows that the yield of regenerated cellulose increased remarkably with the increasing CO₂ pressure less than 6.6 MPa (6.6 MPa are approach to the phase transformation of CO₂ at 25 °C), and then increased slightly when the pressure exceeded 6.6 MPa. Similarly, the DP value of the regenerated cellulose decreased gradually with the increasing pressure by two stages, which also had decreased slowly above 6.6 MPa. It illustrates that more regenerated cellulose was precipitated at higher pressures, especially for the cellulose with relatively lower molecular weight.

Particular care should be taken that the DP value of the regenerated cellulose changes significantly with CO₂ pressure. In our experiment, the pressure of compressed CO₂ was controlled in the range of 2-20 MPa. The DP values of the cellulose precipitated from IL were in the range of 162-233. The most significantly change occurred at 6-6.6 MPa, which had DP values of 215 (6 MPa) and 202 (6.6 MPa) respectively. The cellulose (with degradation definitely in the dissolution process) in the IL

can be staged by control of the pressure of gas anti-solvent. This was very different from the anti-solvent reaction in ethanol, which cannot separate the cellulose with different DP, and indicated that the staged bio-refinery of cellulose from IL systems can be easily realized by using compressed CO₂ as anti-solvent.

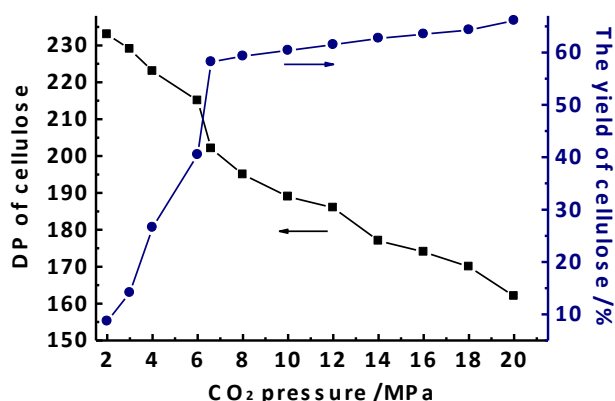


Fig. 2 The DP value and yield of the regenerated cellulose obtained by using compressed CO₂ during a 3 h anti-solvent reaction under different pressure at 25°C.

The effects of the temperature on the anti-solvent reaction at a given compressed CO₂ pressure (10 MPa) and reaction time 3 h were also investigated. The yields of regenerated cellulose were 64.2 % (DP = 184) at 15 °C, 60.4 % (DP = 189) at 25 °C, and 58.9 % (DP = 190) at 40 °C, respectively (Fig. 3). A higher temperature did not benefit the extraction of cellulose due to the lower density and the weaker solvation strength of CO₂ at higher temperature under the certain pressure. It was difficult for the short chain cellulose to be precipitated from the system, so the average DP value of the regenerated cellulose became higher at high temperature.

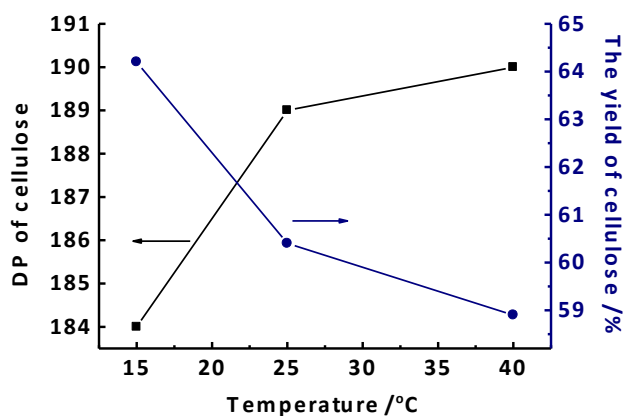


Fig. 3 The DP value and yield of the regenerated cellulose obtained by using compressed CO₂ during a 3 h anti-solvent reaction under a pressure of 10 MPa at 15, 25, and 40 °C.

Influence of co-solvent on the anti-solvent process

As reported in the literatures,⁵⁶⁻⁵⁸ addition of a co-solvent has significantly influence on the solubility of cellulose in IL. In addition to some desired advantages like low viscosity, high dissolution speed and non-derivatization, the prominent feature of the novel systems is that cellulose can be easily dissolved at relatively mild condition with high solubility. It is known that these co-solvents are aprotic polar solvents, which can be speculated that addition of them in IL will result in the further dissociation of IL to produce more solvated cations and free anions, providing more opportunities to interact with cellulose.⁵⁶

Based on these information, the compressed CO₂ anti-solvent on the systems of [Bmim]OAc/co-solvent (1:1(w/w))/MCC (10 wt%) with three kinds of aprotic polar solvents, including DMSO, DMI, and *N,N*-dimethylformamide (DMF), were investigated. Table S1 shows that more cellulose could be regenerated from the IL/co-solvent/MCC systems than the neat IL/MCC system in the same reaction time by using compressed CO₂ (6.6 MPa, 25 °C) as anti-solvent, and using DMSO was the most striking. Additionally, the lower DP of regenerated cellulose can be precipitated from the systems with co-solvent.

In order to verify the influence of co-solvent on the cellulose precipitation, some analysis was further investigated. Fig. 4 shows the dependence of the yield and DP value of regenerated cellulose from the system of [Bmim]OAc/DMSO (1:1(w/w))/MCC (10 wt%) with CO₂ pressure. Adding co-solvent in the IL/MCC displayed high reaction rate for the regenerated cellulose and it took only 2 h to reach equilibrium. It can be also found that the regenerated cellulose yield increased slowly above 6.6 MPa, while the products can be staged more fine with different DP values. The DP values of the cellulose were in the range of 157-175 obtained at CO₂ pressure of 6.6-20 MPa, which indicated that one could get regenerated cellulose with narrow molecular weight distribution when adding DMSO in the systems. Fig. S2 and Fig. S3 reveal that DMI and DMF have similar effects as DMSO.

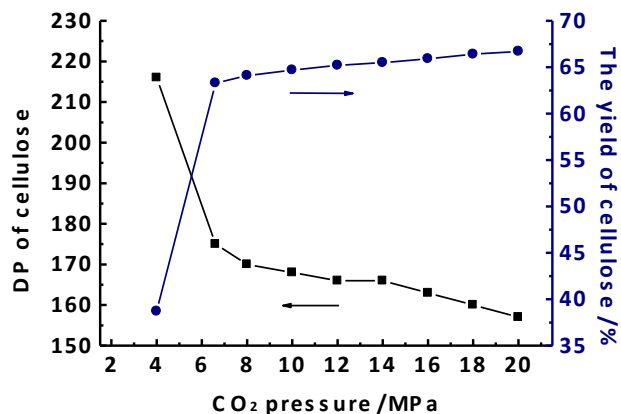


Fig. 4 The DP value and yield of the regenerated cellulose obtained from the system of [Bmim]OAc/DMSO (1:1(w/w))/MCC (10 wt%) by using compressed CO₂ during a 3 h anti-solvent reaction under different pressure at 25°C.

The mechanisms of precipitation and staged bio-refinery of cellulose

The above results show that reaction time, pressure, temperature and co-solvent are all main factors affecting the cellulose precipitation and staged bio-refinery process. We then attempted to explain the possible reasons. CO₂ is a non-polar molecule, and it has a strong quadrupolar moment arising from two opposed dipoles in the linear molecule,⁵⁹⁻⁶⁰ which allows for strong interactions with the cations and anions of IL. [Bmim]OAc can be used to capture CO₂ efficiently. The chemical absorption of CO₂ with [Bmim]OAc may form the carboxylate zwitterions,^{48, 61} leading to the disruption of the hydrogen bonding between cellulose and IL, and also compete for solubilizing acetate anions, thus resulting in precipitation of cellulose from [Bmim]OAc.

To explore the species changes in this system further, we compare the ¹H and ¹³C NMR spectra of [Bmim]OAc before and after charging CO₂ (Fig. 5A and 5B). ¹H NMR has been used to confirm the formation of the carboxylate zwitterions imidazolium-2-carboxylate ([Bmim⁺-COO⁻]).⁴⁸ The proton decoupled ¹³C spectra were also displayed to compare with the differences between the [Bmim]OAc and the mixture of [Bmim]OAc/CO₂. We can observe that a new ¹³C resonance at 152.85 ppm after charging CO₂. Since the isolated CO₂ has a single resonance at 125.4 ppm,⁶² the new resonance cannot correspond to the CO₂ molecule that dissolved into IL directly. Therefore, it can be attributed to the reaction between [Bmim]OAc and CO₂. The acidic proton at C(2) may take place a chemical exchange from the imidazolium ring to the acetate anion,⁶³ and the addition of CO₂ can disturb the equilibrium by the carboxylation reaction, leading to the formation of a CO₂-carbene intermediate and the new species of [Bmim⁺-COO⁻].

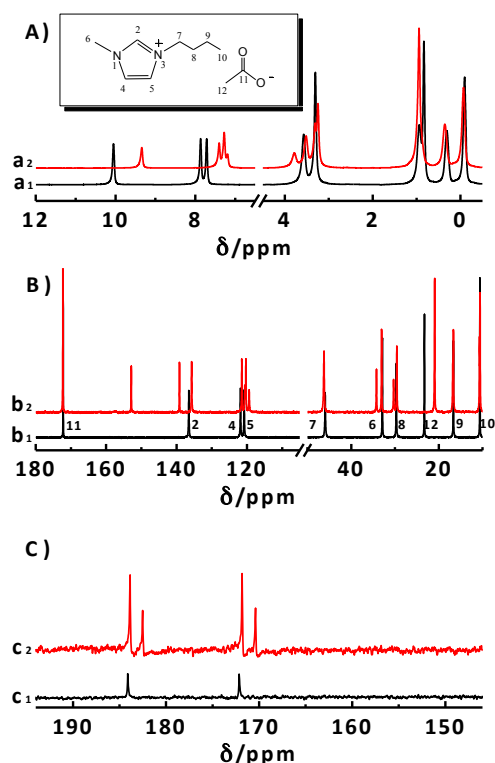


Fig. 5 ¹H (A), ¹³C (B) and ¹⁵N (C) NMR spectra of [Bmim]OAc without (a₁, b₁ and c₁) and with charging CO₂ (a₂, b₂ and c₂) at 25°C.

To prove this point further, we measured the ¹⁵N NMR spectra of pure [Bmim]OAc and the mixture of [Bmim]OAc/CO₂ (Fig. 5C). For pure [Bmim]OAc, the spectrum presents two resonances at 172.13 and 184.10 ppm assigned to the nitrogen atoms of the imidazolium ring. However, in the mixture of [Bmim]OAc/CO₂, two additional ¹⁵N resonances upfield shifting each of the previous resonances can be observed at 170.37 and 182.49 ppm. It indicated that another chemical environment was formed for the nitrogen atoms on the imidazolium ring after charging CO₂. Combined with the previous ¹³C NMR, the carboxylation reaction at the position of C(2) may form [Bmim⁺-COO⁻] and increase the electron cloud density around the nitrogen atoms, which also supports our previous conclusion concerning the chemical reaction between [Bmim]OAc and CO₂. In addition, it is noted that the ratio of integral relative peak area of two ¹⁵N resonances for the [Bmim]⁺ and [Bmim⁺-COO⁻] is 4:1. That is to say, 1 mol IL may fix 0.2 mol CO₂, which approaches the greatest amount of CO₂ uptake of [Bmim]OAc under atmosphere pressure at 25 °C. It can be concluded that the interaction site of hydrogen bonds of [Bmim]OAc can combine CO₂ molecule prior to the cellulose. Overall, the chemical interaction between [Bmim]OAc and CO₂ can greatly improve the precipitation of cellulose from IL.

On the other hand, the volume expansion of IL caused by compressed CO₂ may impel the distance between cellulose and IL to move longer. The attractive intermolecular force of the compressed CO₂ might drive the cellulose molecule to a more favorable region. The cellulose molecule may be distributed abundantly around by CO₂ and promote the separation from IL. In the anti-solvent process, the cellulose with long chain and large molecular weight has more opportunities to be surrounded by CO₂, as well as the poor interaction with IL, so it can be precipitated easily. As the anti-solvent interaction of compressed CO₂ can be tuned by control of the temperature, pressure and reaction time, cellulose with different DP values can be obtained and the staged bio-refinery of cellulose may be accomplished successfully.

Furthermore, the regenerated cellulose can be also precipitated from the systems if an aprotic polar solvent is added into [Bmim]OAc. Fig. 6 shows that the systems of [Bmim]OAc/co-solvent/cellulose expanded significantly than that of [Bmim]OAc/cellulose after dissolution of CO₂. The volume expansion ratio obtained in this study and dipole moment of the aprotic polar solvents according to literature⁶⁴ follow the order: DMSO > DMI > DMF. Some previous reports have shown that the solubility of cellulose in IL can be enhanced by adding the aprotic polar solvent.^{56, 65} This research reveals that using compressed CO₂ as anti-solvent the addition of aprotic polar solvent in IL also contributes to the precipitation of cellulose. The three-dimensional hydrogen-bonded network in the pure [Bmim]OAc can be disrupted by addition of the aprotic polar solvents,^{56, 66} leading to present more free OAc⁻ anions and solvation of [Bmim]⁺ cations. The discrete units in the IL can provide more opportunities to interact with CO₂ molecules. So the solution can be expanded more significant after charging CO₂ in the system of [Bmim]OAc/co-solvent. The longer distance between cations and anions caused by compressed CO₂ at the high pressure can make the regenerated cellulose precipitate from

the system of [Bmim]OAc with co-solvent more easily and rapidly than the pure IL.

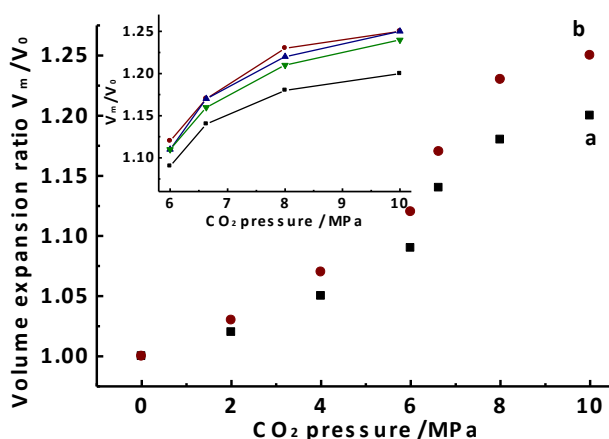


Fig. 6 The volume expansion ratio (V_m/V_0) of 10.0 wt% MCC/[Bmim]OAc (a) and 10.0 wt% MCC/[Bmim]OAc/DMSO (b) solution at 25 °C after charging compressed CO_2 . The inset in figure shows the influence of co-solvent on the volume expansion ratio of 10.0 wt% MCC/[Bmim]OAc solution; from bottom to top is no co-solvent adding, adding DMF, DMI, and DMSO, respectively.

Additionally, we present a survey of Kamlet–Taft solvatochromic parameters, which are the most comprehensive and frequently used quantitative measure of solvent properties.⁶⁷ Our previous studies⁴⁷ indicate that the addition of CO_2 in neat [Bmim]OAc caused a relatively obvious decrease in polarity/polarizability (π^*) but a slightly change in the hydrogen basicity (β) and acidity (α). In this part, we examine the effect of adding DMSO/DMI/DMF into [Bmim]OAc on these parameters as a function of CO_2 pressure. The amount of probe molecules partitioning into the CO_2 fluid phase is negligible. The pressure-dependent data for three kinds of [Bmim]OAc/co-solvent (1:1(w/w)) at 25 °C are shown in Fig. 7. Fig. 7A shows that the π^* of [Bmim]OAc/co-solvent decreased significantly with the increasing CO_2 pressure, which is similar as that of pure [Bmim]OAc. The π^* value of [Bmim]OAc/DMSO decreased from 0.907 to 0.857 at 25 °C, as the CO_2 pressure increased from 0 to 20 MPa, which were remarkably higher than those of [Bmim]OAc/DMI and [Bmim]OAc/DMF, but were lower than that of [Bmim]OAc. It followed the same order as dipole moment of the aprotic polar solvents. The polarity of system with aprotic polar solvent changed little, which could be used to explain the relatively narrow molecular weight distribution and DP values of regenerated cellulose by compressed CO_2 .

Fig. 7B, 7C, and 7D demonstrate the effect of CO_2 on the β , α , and ($\beta-\alpha$) values for [Bmim]OAc/co-solvent (1:1(w/w)) at 25 °C, which represent the hydrogen bond accepting ability, donating ability, and net basicity, respectively. The β values were dependent on the co-solvent, and the pressure of CO_2 had little effect on β values for all the systems studied. Compared with the results for pure [Bmim]OAc previously reported,⁴⁷ the α values were all much lower and increased with the increasing pressure, with DMF was the most significant one. When combined it with β values, a similar order can obtain as the order of π^* . It indicated that CO_2 molecule can interaction with the cations and anions of

IL through hydrogen bonds to some extent. Meanwhile, the high ($\beta-\alpha$) values can be viewed as the evidence of high ability of cellulose dissolution, leading to incomplete precipitation of cellulose by using compressed CO_2 as anti-solvent.

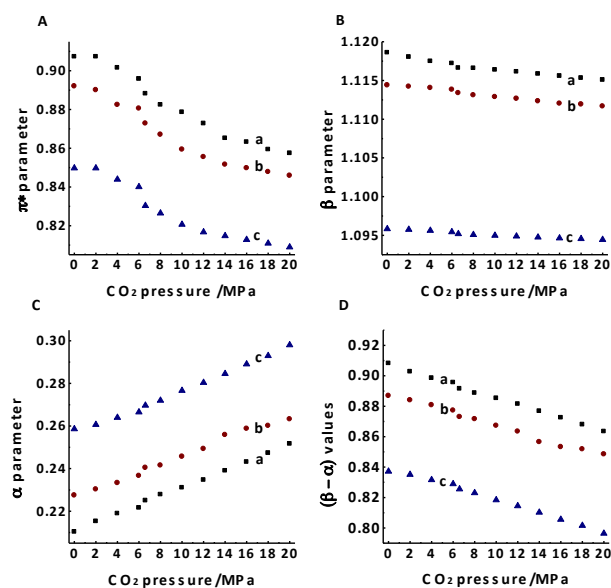


Fig. 7 Kamlet-Taft parameters for [Bmim]OAc/ CO_2 mixtures with different co-solvents adding at 25 °C under different pressure, including adding DMSO (a), DMI (b) and DMF (c), respectively.

Characterization of the regenerated cellulose

Then, the cellulose samples regenerated from [Bmim]OAc using different anti-solvents were characterized. The CP/MAS ^{13}C NMR spectra of the samples are shown in Fig. 8. The spectrum of the native cellulose is typical of cellulose I, and the signals at 89.3 and 65.7 ppm correspond to the C(4) and C(6) of crystalline cellulose, respectively.⁶⁸⁻⁷⁰ The regenerated cellulose samples obtained from both compressed CO_2 and ethanol were transformed into the typical of cellulose II. It was noted that the signal attributed to C(4) of crystalline cellulose almost disappeared as compared with the native one, which indicated that the crystallinity dramatically decreased due to the dissolution and anti-solvent treatment processes.

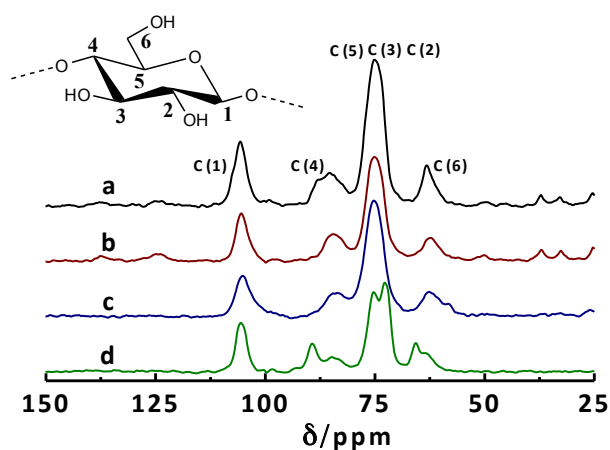


Fig. 8 ^{13}C CP/MAS spectra of the cellulose samples: a) the regenerated cellulose by compressed CO_2 under 6.6 MPa; b) the regenerated cellulose by compressed CO_2 under 20.0 MPa; c) the regenerated cellulose by ethanol; d) the native cellulose.

Fig. 9 shows the XRD profiles of the native and regenerated cellulose from the solution of [Bmim]OAc/cellulose (10.0 wt%). It is noted that the native cellulose shows a better diffraction pattern (with obvious peaks at $2\theta = 15.4, 22.4$ and 34.4 degrees) than the regenerated cellulose (only a large broad amorphous at $2\theta = 19.8$ degree), which suggests that the regenerated cellulose has less crystallization degree than the native one. Two possible reasons can be used to explain the phenomenon: one is that some of the intrinsic inter- and intra- molecular hydrogen bonds and the crystalline formation have been destroyed in the process of dissolution in [Bmim]OAc; the other is the methods of the regenerated cellulose using compressed CO_2 or ethanol cannot reconstituted the structure of crystallization.

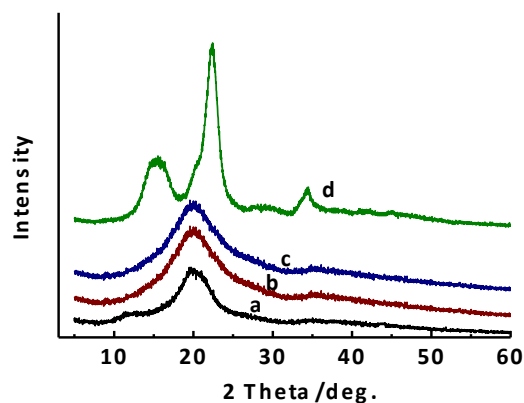


Fig. 9 XRD patterns of the cellulose samples: a) the regenerated cellulose by compressed CO_2 under 6.6 MPa; b) the regenerated cellulose by compressed CO_2 under 20.0 MPa; c) the regenerated cellulose by ethanol; d) the native cellulose.

AFM images of the regenerated and native cellulose from [Bmim]OAc are shown in Fig. 10. The native cellulose shows a heterogeneous texture (Fig. 10A), while the regenerated ones indicate a much more uniform morphology. On the other hand,

the thickness of samples becomes thinner obviously after regeneration, which is consistent with DP findings of the samples. Unlike the loose architecture of that precipitated by ethanol (Fig. 10B), the regenerated cellulose obtained by compressed CO_2 shows much higher density and the inerratic and crimped surface (Fig. 10C, 10D). Additionally, it is worth noting that the pressure of CO_2 affects the morphology of the regenerated cellulose. As the increase of pressure, the homogeneous structure can be changed from flocculent products (Fig. 10C) to the fiber-like pieces (Fig. 10D). We can conclude that the regenerated cellulose from IL is breathable and remains intact when using compressed CO_2 as anti-solvent.

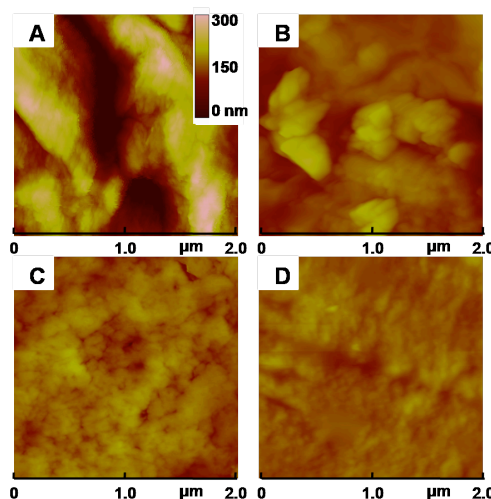


Fig. 10 AFM images of the cellulose samples: A) the native cellulose; B) the regenerated cellulose by ethanol; C) the regenerated cellulose by compressed CO_2 under 6.6 MPa; D) the regenerated cellulose by compressed CO_2 under 20.0 MPa.

Energy consumption comparison with different anti-solvents

Conventional anti-solvent method using high boiling-point solvents (e.g., ethanol, dichloromethane, water) has been widely applied in regenerating cellulose. However, the used solvents might cause environmental issues and additional processes are demanded for the IL recovery and purification, which might result in the increase of the production cost. By comparison, compressed CO_2 is well-suited for regenerated cellulose as anti-solvent. We gave an approximate evaluation on the energy consumption of the cellulose precipitation from IL by ethanol and compressed CO_2 as anti-solvent, and the results were given in the Electronic Supplementary Information. The results showed that the compressed CO_2 consumed is more energy saving than ethanol in the anti-solvent process for cellulose precipitation from IL, and it offers facile solvent removal solely by depressurization.

Conclusions

In summary, an easy and efficient method to precipitate cellulose from IL using compressed CO_2 as gas anti-solvent was designed. The yield and DP values of the regenerated cellulose can be finely tuned by control of the temperature, pressure, reaction time, and addition of aprotic polar solvents. Generally, it is found that the yield of regenerated cellulose is increasing and the average DP value is decreasing with the increasing of reaction time until

the regeneration process is carried out completely. The increasing pressure, the decreasing temperature and adding aprotic polar co-solvent may all contribute to precipitate the lower molecular products, leading to reduce the average DP value of the regenerated cellulose. In this process, the carboxylation reaction between [Bmim]OAc and CO₂ can be detected, which helps the precipitation of cellulose from IL. In the meantime, the solvent strength of the certain system can be regulated by the condition of CO₂ loading, including the volume expansion of the solution and reducing the polarity and net donating ability of hydrogen bonds, which indicated that CO₂ may occupy the initial space between cations and anions of IL instead of cellulose. In addition, the regenerated cellulose from the IL by compressed CO₂ has some specificity, which overcomes the drawbacks of the native cellulose or the regenerated cellulose using some conventional anti-solvent systems. Combined with the energy consumption comparison, it can be concluded that compressed CO₂ anti-solvent may provide us an easy, sustainable and cost-efficient method for regeneration and staged bio-refinery of cellulose from IL.

Experimental

Materials

The microcrystalline cellulose (MCC) was purchased from Sigma Aldrich (St. Louis, U.S.A.). The cellulose samples used were dried in vacuum at 100 °C for about 12 h. N₂ (99.999%) and CO₂ (99.995%) were purchased from Beijing Huayuan Gas Chemical Industry Co., Ltd. (Beijing, China). [Bmim]OAc with a purity over 99.9 wt% was purchased from Lanzhou Greenchem. ILs, LICP, CAS, China (Lanzhou, China). The water contents of IL was determined by Karl-Fischer titration after drying it at 40 °C under vacuum conditions for 96 h, and it has a water content less than 1000 ppm. The standard reagent of 1 mol/L copper (II)-ethylenediamine (Cuen) solution in water was purchased from Acros Organics.

Dissolution of MCC in IL and IL/co-solvents

Under the continuous stirring, finely grinding MCC powder (0.1 wt% of the IL) was added into a flask with about 5.0 g dried [Bmim]OAc at 110 °C under a nitrogen atmosphere. Additional MCC (another 0.1 wt% of the IL) was added until the solution became clear. Considerable repeated operation was needed to add into the system until the concentration of MCC reached 10.0 wt% of the [Bmim]OAc. The MCC/[Bmim]OAc/co-solvents solution with 10 wt% MCC were also obtained via the same method.

Recovery of cellulose from IL and IL/co-solvents by compressed CO₂

The apparatus consisted of a high-pressure view cell with a 20-50 ml variable volume, a water bath with a constant temperature controller (± 0.1 °C), a high-pressure syringe pump (DB-80), a gas cylinder, a magnetic stirrer, and a pressure gauge (± 0.025 MPa) in the pressure range of 0-22 MPa. In a typical experiment, 1 g MCC solution was loaded into the view cell and then was placed in the water bath with the desired temperature. After removing the air, CO₂ was charged into the cell until the thermal equilibrium had been reached. The system was kept up under certain conditions for several hours and then removed it under vacuum to exhaust CO₂. The isolated yields of regenerated MCC can be calculated after washing the aerogels completely by

ethanol. The DP of cellulose samples that dissolved in the standard reagent of 1 mol/L (Cuen), were then determined by intrinsic viscosity measurement using an Ubbelohde viscometer.

NMR measurements of pure IL and IL/CO₂ system

The binary system of IL [Bmim]OAc and CO₂ was prepared by loading the dried IL in the high-pressure view cell, and charging CO₂ into the cell (6.6 MPa at 25 °C). After it was kept to equilibrate for at least 12 h, redundant CO₂ was removed and the pressure released to the normal pressure (0.1 MPa). The NMR samples were measured as neat liquids using co-axial capillary containing D₂O as a lock solution. ¹H NMR and ¹³C NMR measurements were performed on a Bruker DMX 300 spectrometer operating at 300 MHz for ¹H and 75 MHz for ¹³C. ¹⁵N NMR spectra of samples were acquired with a Bruker Avance 600 MHz spectrometer operating at 60 MHz.

Measurement of solvatochromic parameters of IL/co-solvent mixtures at different pressures

The apparatus and processor to determine the solvatochromic parameters were similar with previous reports.⁷¹⁻⁷⁴ Briefly speaking, the UV-vis absorbance spectrum of [Bmim]OAc and its mixtures with three aprotic polar solvents with three kinds of dyes, *N,N*-diethyl-4-nitro-aniline (DNA), 4-nitroaniline (NA) and Reichardt's dye 33, were recorded by a TU-1201 Model spectrophotometer (Beijing General Instrument Company) under different CO₂ pressures. The maximum absorption wavelengths (λ_{\max}) of the dyes were used to calculate the solvatochromic parameters (π^* , α and β), and the λ_{\max} stated was the average of three separate scans.

Characterization of the regenerated and native cellulose

CP/MAS ¹³C NMR spectra were obtained at 100.4 MHz using a Bruker Avance III 400M spectrometer. The crystal phases of the regenerated and native cellulose film samples were determined by XRD (Rigaku D/max-2500) using Cu K α as X-ray radiation under 40 kV and 200 mA. The scanning range is $2\theta = 5-60^\circ$ with a step of $2\theta = 0.02^\circ$ and 0.5 s per step. AFM images of cellulose samples were obtained in the tapping mode with a silicon tip under ambient conditions, a scanning rate of 1 Hz, and a scanning line of 512 using the Veeco D3100 instrument (Veeco Instruments 151 Inc., USA).

Acknowledgments

The authors thank the National Natural Science Foundation of China (21173267) for financial support.

Notes and references

^a Department of Chemistry, Renmin University of China, Beijing 100872, China. Tel : 8610-62514925, Email: tcmu@chem.ruc.edu.cn

^b Materials Science and Engineering College, Northeast Forestry University, Harbin, 150040, China

[†] Electronic Supplementary Information (ESI) available: some of the relevant results and discussion. See DOI: 10.1039/b000000x/

1. A. Pinkert, K. N. Marsh, S. Pang and M. P. Staiger, *Chem. Rev.*, 2009, **109**, 6712-6728.
2. P. Weerachanchai and J.-M. Lee, *ACS Sustainable Chem Eng.*, 2013, **1**, 894-902.
3. L. Caspeta, N. A. A. Buijs and J. Nielsen, *Energy Environ Sci.*, 2013, **6**, 1077-1082.

4. M. He, Y. Sun and B. Han, *Angew. Chem. Int. Ed.*, 2013, **52**, 9620-9633.
5. A. L. Marshall and P. J. Alaimo, *Chem. Eur. J.*, 2010, **16**, 4970-4980.
6. A. Corma, S. Iborra and A. Velty, *Chem. Rev.*, 2007, **107**, 2411-2502.
7. G. W. Huber, S. Iborra and A. Corma, *Chem. Rev.*, 2006, **106**, 4044-4098.
8. M. E. Himmel, S.-Y. Ding, D. K. Johnson, W. S. Adney, M. R. Nimlos, J. W. Brady and T. D. Foust, *Science*, 2007, **315**, 804-807.
9. S. Hu, Z. Zhang, J. Song, Y. Zhou and B. Han, *Green Chem.*, 2009, **11**, 1746-1749.
10. J. L. Song, H. L. Fan, J. Ma and B. X. Han, *Green Chem.*, 2013, **15**, 2619-2635.
11. S. Hu, Z. Zhang, Y. Zhou, J. L. Song, H. L. Fan and B. X. Han, *Green Chem.*, 2009, **11**, 873-877.
12. J. Li, D. J. Ding, L. Deng, Q. X. Guo and Y. Fu, *ChemSusChem*, 2012, **5**, 1313-1318.
13. R. Rinaldi and F. Schuth, *ChemSusChem*, 2009, **2**, 1096-1107.
14. X. Hu and C. Z. Li, *Green Chem.*, 2011, **13**, 1676-1679.
15. J. Sanders, E. Scott, R. Weusthuis and H. Mooibroek, *Macromol. Biosci.*, 2007, **7**, 105-117.
16. Q. Zhang, M. Benoit, K. D. O. Vigier, J. Barrault, G. Jégou, M. Philippe and F. Jérôme, *Green Chem.*, 2013, **15**, 963-969.
17. D. Klemm, B. Heublein, H. P. Fink and A. Bohn, *Angew. Chem. Int. Ed.*, 2005, **44**, 3358-3393.
18. A. W. T. King, J. Asikkala, I. Mutikainen, P. Jarvi and I. Kilpelainen, *Angew. Chem. Int. Ed.*, 2011, **50**, 6301-6305.
19. R. P. Swatloski, S. K. Spear, J. D. Holbrey and R. D. Rogers, *J. Am. Chem. Soc.*, 2002, **124**, 4974-4975.
20. H. Wang, G. Gurau and R. D. Rogers, *Chem. Soc. Rev.*, 2012, **41**, 1519-1537.
21. A. Xu, J. Wang and H. Wang, *Green Chem.*, 2010, **12**, 268-275.
22. S. Fischer, W. Voigt and K. Fischer, *Cellulose*, 1999, **6**, 213-219.
23. T. Heinze and T. Liebert, *Prog. Polym. Sci.*, 2001, **26**, 1689-1762.
24. C. L. McCormick and T. R. Dawsey, *Macromolecules*, 1990, **23**, 3606-3610.
25. P. Wasserscheid and W. Keim, *Angew. Chem. Int. Ed.*, 2000, **39**, 3772-3789.
26. J. P. Hallett and T. Welton, *Chem. Rev.*, 2011, **111**, 3508-3576.
27. T. Welton, *Chem. Rev.*, 1999, **99**, 2071-2083.
28. M. Petkovic, K. R. Seddon, L. P. N. Rebelo and C. S. Pereira, *Chem. Soc. Rev.*, 2011, **40**, 1383-1403.
29. M. Armand, F. Endres, D. R. MacFarlane, H. Ohno and B. Scrosati, *Nat. Mater.*, 2009, **8**, 621-629.
30. S. D. Zhu, Y. X. Wu, Q. M. Chen, Z. N. Yu, C. W. Wang, S. W. Jin, Y. G. Ding and G. Wu, *Green Chem.*, 2006, **8**, 325-327.
31. J. B. Binder and R. T. Raines, *J. Am. Chem. Soc.*, 2009, **131**, 1979-1985.
32. H. Zhang, J. Wu, J. Zhang and J. S. He, *Macromolecules*, 2005, **38**, 8272-8277.
33. N. Luo, Y. Lv, D. Wang, J. Zhang, J. Wu, J. He and J. Zhang, *Chem. Commun.*, 2012, **48**, 6283-6285.
34. H. Song, Y. Niu, J. Yu, J. Zhang, Z. Wang and J. He, *Soft Matter*, 2013, **9**, 3013-3020.
35. J. S. Moulthrop, R. P. Swatloski, G. Moyna and R. D. Rogers, *Chem. Commun.*, 2005, 1557-1559.
36. H. T. Vo, Y. J. Kim, E. H. Jeon, C. S. Kim, H. S. Kim and H. Lee, *Chem. Eur. J.*, 2012, **18**, 9019-9023.
37. Q. T. Chen, A. R. Xu, Z. Y. Li, J. J. Wang and S. J. Zhang, *Green Chem.*, 2011, **13**, 3446-3452.
38. W. N. Liu, Y. C. Hou, W. Z. Wu, S. H. Ren, Y. Jing and B. G. Zhang, *Ind. Eng. Chem. Res.*, 2011, **50**, 6952-6956.
39. E. S. Hassan, F. Mutelet, S. Pontvianne and J. C. Moise, *Environ. Sci. Technol.*, 2013, **43**, 2809-2816.
40. L. A. Blanchard, D. Hancu, E. J. Beckman and J. F. Brennecke, *Nature*, 1999, **399**, 28-29.
41. B. Wu, W. Liu, Y. Zhang and H. Wang, *Chem. Eur. J.*, 2009, **15**, 1804-1810.
42. J. L. Zhang, B. X. Han, C. Zhang, W. Li and X. Feng, *Angew. Chem. Int. Ed.*, 2008, **47**, 3012-3015.
43. J. L. Zhang, B. X. Han, J. C. Liu, X. G. Zhang, J. He, Z. M. Liu, T. Jiang and G. Y. Yang, *Chem. Eur. J.*, 2002, **8**, 3879-3883.
44. J. L. Zhang and B. X. Han, *J. Supercrit. Fluids*, 2009, **47**, 531-536.
45. B. R. Mellein and J. F. Brennecke, *J. Phys. Chem. B*, 2007, **111**, 4837-4843.
46. Y. P. Sun, M. J. Mezziani, P. Pathak and L. Qu, *Chem. Eur. J.*, 2005, **11**, 1366-1373.
47. X. Sun, Z. Xue and T. Mu, *Green Chem.*, 2014, DOI: 10.1039/C3GC42166J.
48. P. S. Barber, C. S. Griggs, G. Gurau, Z. Liu, S. Li, Z. Li, X. Lu, S. Zhang and R. D. Rogers, *Angew. Chem.*, 2013, **125**, 12576-12579.
49. P. G. Jessop and B. Subramaniam, *Chem. Rev.*, 2007, **107**, 2666-2694.
50. J. W. Ford, M. E. Janakat, J. Lu, C. L. Liotta and C. A. Eckert, *J. Org. Chem.*, 2008, **73**, 3364-3368.
51. C. P. Fredlake, M. J. Muldoon, S. N. V. K. Aki, T. Welton and J. F. Brennecke, *Phys. Chem. Chem. Phys.*, 2004, **6**, 3280-3285.
52. A. P. Abbott, E. G. Hope, R. Mistry and A. M. Stuart, *Green Chem.*, 2009, **11**, 1530-1535.
53. A. R. Xu, J. J. Wang and H. Y. Wang, *Green Chem.*, 2010, **12**, 268-275.
54. H. Zhao, G. A. Baker, Z. Song, O. Olubajo, T. Crittle and D. Peters, *Green Chem.*, 2008, **10**, 696-705.
55. H. M. Cho, A. S. Gross and J. W. Chu, *J. Am. Chem. Soc.*, 2011, **133**, 14033-14041.
56. Y. L. Zhao, X. M. Liu, J. J. Wang and S. J. Zhang, *J. Phys. Chem. B*, 2013, **117**, 9042-9049.
57. K. Ohira, K. Yoshida, S. Hayase, and T. Itoh, *Chem. Lett.*, 2012, **41**, 987-989.
58. A. R. Xu, Y. J. Zhang, Y. Zhao and J. J. Wang, *Carbohydr. Polym.*, 2013, **92**, 540-544.
59. J. F. Kauffman, *J. Phys. Chem. A*, 2001, **105**, 3433-3442.
60. M. Battaglia, A. Buckingham, D. Neumark, R. Pierens and J. Williams, *Mol. Phys.*, 1981, **43**, 1015-1020.
61. G. Gurau, H. Rodriguez, S. P. Kelley, P. Janiczek, R. S. Kalb and R. D. Rogers, *Angew. Chem. Int. Ed.*, 2011, **50**, 12024-12026.
62. M. H. O'Leary, R. J. Jaworski and F. C. Hartman, *Proc. Natl. Acad. Sci. USA*, 1979, **76**, 673-675.

63. M. Besnard, M. I. Cabaco, F. V. Chavez, N. Pinaud, P. J. Sebastiao, J. A. P. Coutinho, J. Mascetti and Y. Danten, *J. Phys. Chem. A*, 2012, **116**, 4890-4901.
64. R. Fernandez-Prini, by AK Covington and T. Dickinson, *Plenum Press, London*, 1973.
65. R. Rinaldi, *Chem. Commun.*, 2011, **47**, 511-513.
66. T. Peppel, C. Roth, K. Fumino, D. Paschek, M. Köckerling and R. Ludwig, *Angew. Chem. Int. Ed.*, 2011, **50**, 6661-6665.
67. J. Lu, C. L. Liotta and C. A. Eckert, *J. Phys. Chem. A*, 2003, **107**, 3995-4000.
68. X. Liu, J. H. Pang, X. M. Zhang, Y. Y. Wu and R. C. Sun, *Cellulose*, 2013, **20**, 1391-1399.
69. S. Raymond, Å. Kvick and H. Chanzy, *Macromolecules*, 1995, **28**, 8422-8425.
70. F. Kolpak and J. Blackwell, *Macromolecules*, 1976, **9**, 273-278.
71. L. K. J. Hauru, M. Hummel, A. W. T. King, I. Kilpelainen and H. Sixta, *Biomacromolecules*, 2012, **13**, 2896-2905.
72. C. Reichardt, *Green Chem.*, 2005, **7**, 339-351.
73. R. Lungwitz and S. Spange, *New J. Chem.*, 2008, **32**, 392-394.
74. A. Oehlke, K. Hofmann and S. Spange, *New J. Chem.*, 2006, **30**, 533-536.